Defect dynamics and strain coupling to magnetization in the cubic helimagnet Cu_2OSeO_3

Donald M. Evans,[1] Jason A. Schiemer,[1] Marcus Schmidt,[2] Heribert Wilhelm,[3] and Michael A. Carpenter[1]
[1]*Department of Earth Sciences, University of Cambridge, Downing Street, Cambridge CB2 3EQ, United Kingdom*
[2]*Max Planck Institute for Chemical Physics of Solids, 01187 Dresden, Germany*
[3]*Diamond Light Source Ltd, Chilton, Didcot, Oxfordshire OX11 0DE, United Kingdom*
(Received 7 December 2016; revised manuscript received 22 January 2017; published 27 March 2017)

Small but significant static and dynamic strain coupling effects have been detected in Cu_2OSeO_3 through elastic and anelastic anomalies associated with magnetic phase transitions observed as a function of temperature (1.5–150 K) and magnetic field (0–300 mT). The magnetic transition near 60 K is accompanied by a small increase in single-crystal elastic constants which can be understood in terms of biquadratic coupling between shear strain and the magnetic order parameter, even though the shear strain itself is almost negligibly small. The conical-collinear transition is associated with distinct minima in the elastic properties, while weaker anomalies at lower fields may be related to changes in the configuration of magnetic domains. A distinctive acoustic loss peak at ∼42 K, independent of magnetic field, is attributed to freezing of a defect which is coupled with shear strain, has an associated activation energy of ∼5 kJ mol^{-1}, and may play a role in pinning the magnetic microstructures. Anomalies below ∼10 K indicate the presence of some additional relaxation process which could signify a change in magnetic structure.

DOI: 10.1103/PhysRevB.95.094426

I. INTRODUCTION

Cu_2OSeO_3 has attracted close attention since the discovery of its multiferroic properties [1] and for the fact that it was the first insulating material in which skyrmions, topologically protected magnetic objects, were observed [2–5]. Both effects are related to the helical magnetism seen below ∼60 K and in fields up to ∼40 mT [2–10]. Magnetoelectric coupling, in the form of an anomaly in the dielectric constant, has been observed for the helical magnetic structures, but there is no evidence of a discrete ferroelectric transition [1,9,11]. On the other hand, although there is no macroscopic electric polarization in zero field, a complex pattern of changing polarization has been observed with increasing magnetic field [2,3,6,9]. Coupling has been seen under the influence of an ac electric field [8] and pronounced magnetoelectric effects have also been observed in the stability field of the skyrmion lattice [2,3,7–10,12,13].

Figure 1 shows the Cu_2OSeO_3 phase diagram as a function of temperature (T) and magnetic field (H). Above $T_c \approx 58$ K, the structure is paramagnetic. At low field strengths the stable magnetic structure is a flat helix, with an incommensurate repeat length of ∼50–70 nm [4,5,14] and propagation vector **q** parallel to a different ⟨100⟩ direction in each of multiple domains. This is referred to either simply as a helical structure or as the "multiple q-domains" structure. According to Seki *et al.* [4] the wave vector does not change in length or direction from T_c down to 10 K. Above some critical field H_{c1}, the flat helix gives way to a conical helix which has a single propagation direction aligned parallel to the applied field ("single q-domain" structure). Finally, above a second critical field H_{c2}, three quarters of the $Cu^{2+}(S = 1/2)$ spin moments become aligned parallel to the field and one quarter antiparallel in a collinear ferrimagnetic structure. A small stability field for the skyrmion lattice occurs close to where the stability limits of all four of the other structures converge.

Spin-lattice coupling in Cu_2OSeO_3 would be expected to give rise to a symmetry-breaking shear strain and the development of ferroelastic twin walls. However, a remarkable feature is that, even though the unique direction of the helical magnetic structure is incompatible with cubic symmetry, no evidence appears to have yet been found that there is any measurable distortion from cubic ($P2_13$) lattice geometry, either at the macroscopic length scale represented by lattice parameters determined by high-resolution x-ray powder diffraction [1], at a phonon length scale [15], or at a local length scale sampled by ^{77}Se nuclear magnetic resonance (NMR) spectroscopy [16]. On the other hand, T_c increases slightly with increasing pressure [17–19], implying the existence of a small negative volume strain. Small variations in the T-H phase diagram near T_c as a function of pressure [19] confirm that subtle magnetoelastic effects extend also to higher magnetic fields.

The most sensitive approach for investigating the strength and dynamics of strain coupling effects is through measurements of elastic and anelastic properties, and the main objective of the present study was to investigate these as simultaneous functions of temperature and magnetic field for Cu_2OSeO_3 using resonant ultrasound spectroscopy (RUS). We have found a number of distinct anomalies through and below T_c which signify a degree of spin-lattice coupling for the helical and conical structures. A small change in shear elastic stiffness occurs at T_c for field strengths between 0 and 220 mT. A Debye-like peak in acoustic loss near 40 K is also present at all field strengths and is attributed to a thermally activated pinning process associated with some as yet undetermined point defects. There is elastic softening below ∼15 K, accompanied by a steep increase in acoustic loss, the cause of which is not understood. When varying field at constant temperature, small but reproducible anomalies coincide with the conical-collinear transition at H_{c2}. Additionally, there are hysteresis effects which occur with varying temperature or field below ∼40 K and are most likely related to changes in magnetic domain patterns. These strain-coupling and relaxation effects are all weak but indicate that strain has a permeating influence

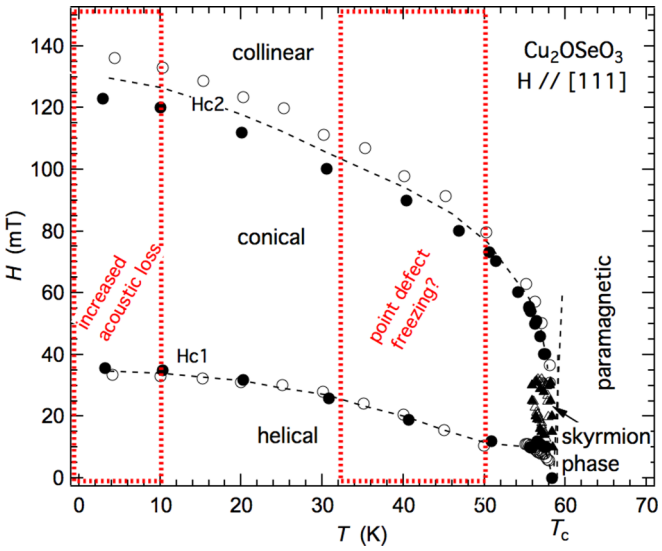

FIG. 1. T-H phase diagram for Cu_2OSeO_3 with the magnetic field aligned parallel to [111], after Adams *et al.* [5] (filled symbols) and Ruff *et al.* [9] (open symbols). Superimposed on the phase diagram are dashed red lines to indicate regions of acoustic loss observed in the present paper.

throughout the fields of stability of the different magnetic structures.

II. EXPERIMENTAL DETAILS

RUS involves measurement of mechanical resonances of small samples held lightly between piezoelectric transducers [20] and provides a highly sensitive method of detecting phase transitions through the influence of strain coupling effects [21]. Individual samples may be single crystals or ceramics with edge dimensions typically in the range ~1–5 mm. Their natural resonances are dominated by shearing motions, with much less from breathing, so that the resonant frequencies are determined primarily by shear elastic constants. Values of the elastic constants which determine each resonant mode scale with f^2. The inverse mechanical quality factor, given by $Q^{-1} = \Delta f/f$, is a measure of acoustic attenuation, where f is the resonant frequency and Δf is the peak width at half maximum height. A cubic crystal has three independent elastic constants which, in symmetry-adapted form, are $\frac{1}{2}(C_{11} - C_{12})$, C_{44}, and the bulk modulus $K = \frac{1}{3}(C_{11} + 2C_{12})$. The observed variations of f^2 are expected to represent the variations of $\frac{1}{2}(C_{11} - C_{12})$ and C_{44} in different proportions, with only small contributions from breathing modes which depend on K.

Spectra reported here were obtained using electronics designed by Dr. A. Migliori in Los Alamos, with a maximum applied voltage of 2 V. The sample holder has been described by McKnight *et al.* [22], though with copper replacing the stainless steel component [23]. The sample holder was lowered into an Oxford Instruments Teslatron cryostat which has a superconducting magnet capable of delivering a magnetic field up to 14 T. Each spectrum consisted of 130 000 data points in the frequency range 0.4–1.2 MHz, collected in automated sequences. In temperature sweeps, the constant field was applied at 1.5 K with measurements taken during heating from 1.5 to 150 K, followed by cooling back to 1.5 K. In field sweeps, temperature was set and measurements were made with increasing field and then decreasing field. A complete list of the sequence is given in the Appendix. The sample space contained a few millibars of helium as exchange gas, and a 10 min settle time was allowed at each set point to allow thermal equilibration.

Single crystals of Cu_2OSeO_3 were grown using a chemical vapor transport reaction and had well-developed crystal faces. The starting material with composition Cu_2OSeO_3 was synthesized by a reaction of CuO (Alfa Aesar 99.995%) and SeO_2 (Alfa Aesar 99.999%) at 300 °C (2 d) and 600 °C (7 d) in evacuated fused silica tubes. The resulting microcrystalline powder material was then recrystallized by chemical transport reaction in a temperature gradient from 575 °C (source) to 460 °C (sink) with HCl as the transport agent. This transport agent had been formed *in situ* in the gas phase by decomposition of NH_4Cl(1 mg/cm^3) into ammonia and HCl. Selected crystals were characterized by Energy-dispersive X-ray spectroscopy (EDXS), x-ray powder, and x-ray single-crystal diffraction. All methods revealed the very high quality of the crystals, and Qian *et al.* [24] have reported a value of the magnetic transition temperature of $T_c = 58.2 \pm 0.05$ K in zero field.

The single crystal used for RUS was an irregular polygon with well-defined growth faces, a maximum dimension of ~1.5–2 mm and mass 1.2 mg. It had the particular advantage of displaying an opposing pair of growth faces parallel to {111} so that when these were placed in direct contact with the transducers of the RUS head the applied magnetic field was exactly parallel to [111].

III. RESULTS

A. Temperature dependence of RUS signal

Segments of primary spectra showing a single resonance peak from Cu_2OSeO_3 in zero magnetic field are given in Fig. 2, where they are stacked in proportion to the temperature at which they were collected. Several features are immediately apparent: a change in trend at ~60 K corresponding to increasing resonance frequencies below T_c (elastic stiffening), peak broadening at ~40–45 K corresponding to increased acoustic loss, decreasing frequency with falling temperature below ~15 K (elastic softening), and a significant increase in peak widths below ~10 K (increasing loss). These changes have been quantified by fitting an asymmetric Lorentzian function to selected peaks in order to extract values of f and Δf.

Figure 3 contains f^2 and Q^{-1} values from fitting of individual resonance peaks within spectra collected during heating and cooling in constant magnetic fields of between 0 and 150 mT. There is a clear change in the trend of f^2 at ~60 K, indicative of a small, continuous increase in elastic stiffness with falling temperature through T_c. The same kink is observed for all the resonances, and the only dependence on magnetic field is a very small shift to higher temperature with increasing field. The resonance peaks themselves do not show any visible broadening through T_c, but fitting to the peak widths reveals what appears to be a very small peak in Q^{-1} in some cases [Figs. 3(a) and 3(b)]. The most obvious

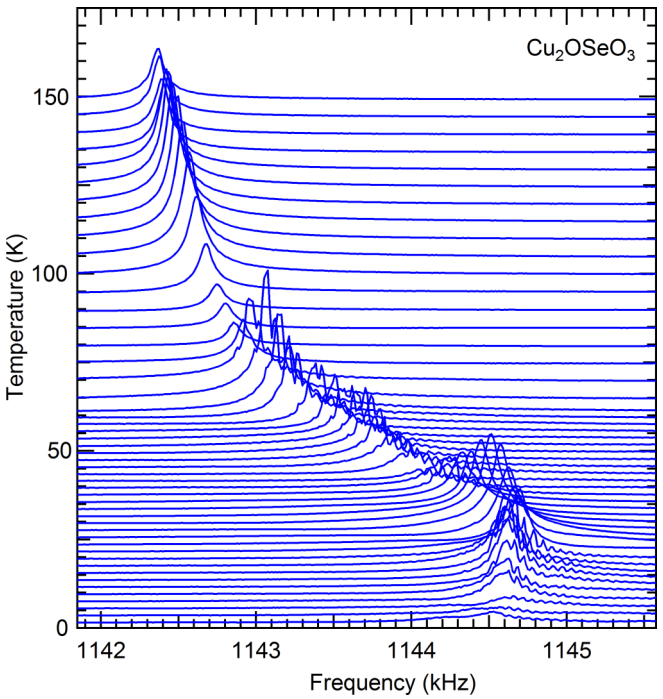

FIG. 2. Segments of RUS spectra of Cu_2OSeO_3 collected during cooling showing a single resonance peak with frequency ~1144 kHz. The y axis was originally amplitude in volts from the detecting transducer, but the spectra have been offset in proportion to the temperature at which they were collected and the axis labeled as temperature.

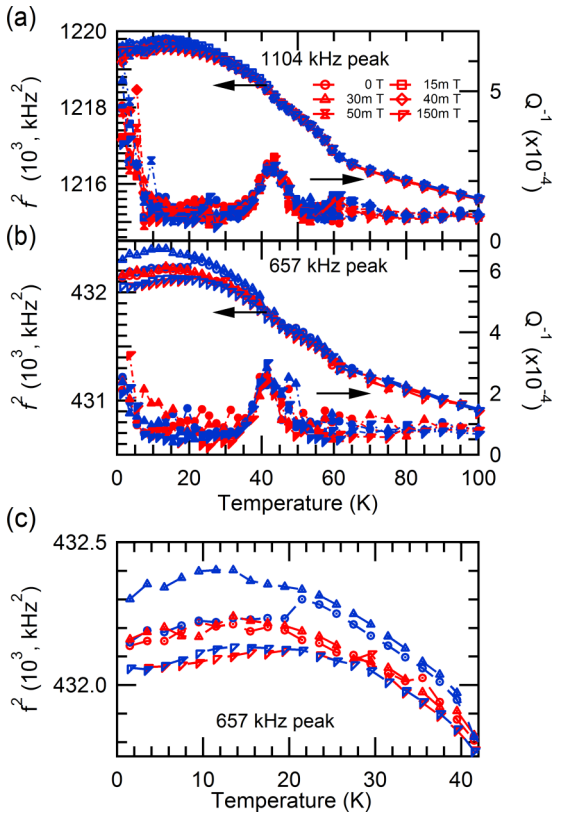

FIG. 3. Variations of f^2 (proportional predominantly to shear elastic constants) and Q^{-1} (indicative of acoustic attenuation) for representative resonances as a function of temperature with different external magnetic field strengths. (a) Resonance peak with frequency close to 1104 kHz. (b) Resonance peak with frequency close to 657 kHz. (c) Magnification of the low-temperature region of (b) showing hysteresis of f^2 values obtained at temperatures below ~42 K: red (heating), blue (cooling).

feature from peak broadening in the primary spectra is a Debye-like peak in Q^{-1} accompanied by a small increase in f^2 at ~42 K. This has the same form for all the resonances examined and, within experimental uncertainty, does not vary with the magnitude of the applied magnetic field. A third clear anomaly is the steep increase in Q^{-1} and slight reduction of f^2 below ~10 K. Finally, hysteresis in f^2 values occurs between heating and cooling for all the resonances below the temperature of the Debye peak in Q^{-1},~42 K, [Fig. 3(c)], but there is no immediate sign of any irreversibility at temperatures higher than this.

B. Field dependence of RUS signal

The unusually high resolution and low noise of the primary spectra are a reflection of the high quality of the Cu_2OSeO_3 single crystal and have allowed details of subtle variations in f^2 and Q^{-1} also to be detected as a function of variable magnetic field at constant temperature. Data for f^2 of a resonance with frequency ~1144 kHz are shown in Fig. 4(a) and display a pattern of softening and stiffening which is representative of all the resonances followed. There is no discernible influence of changing field at 80 K, but at 61 K, there is an almost linear increase (elastic stiffening) with increasing field. At progressively lower temperatures this overall increase reduces in magnitude and an obvious dip (softening) appears. The dip is most pronounced in the data collected at 1.5 K and has a minimum that generally moves to higher fields as temperature is reduced.

Figure 4(b) shows the related data for Q^{-1} from fitting of the same resonance peak as used to obtain the f^2 data in Fig. 4(a). The absolute values obtained at most temperatures were ~1 $\times$ 10^{-4}, signifying extremely low loss. Higher values at 46.5 K correlate with those of the Debye peak seen at ~42 K when varying temperature at constant field and at 1.5 K with the high loss seen at the lowest temperatures (Fig. 3). Small peaks in Q^{-1} at ~95,~110, and ~160 mT in the data collected at 46.5, 5, and 1.5 K, respectively, have the appearance of Debye-like loss behavior, as might occur for some freezing process in which mobile magnetoelastic defects becomes pinned. The magnitudes of the changes are extremely small, however.

The effective temperature and field dependence of elastic softening evident in Fig. 4(a) is seen clearly also in the more comprehensive set of data for five different resonances shown in Fig. 4(c). For this, f^2 values were scaled in such a way that the lowest value at the lowest temperature was set to 1. Each set of peaks, grouped by the temperature at which the spectra were collected, has then been given an arbitrary offset along the y axis. The magnitude of the softening involved and the field at which f^2 is a minimum, $H_{f\,2\mathrm{min}}$, both reduce with increasing temperature, but with slight differences for each of the individual resonances. There is no obvious correlation

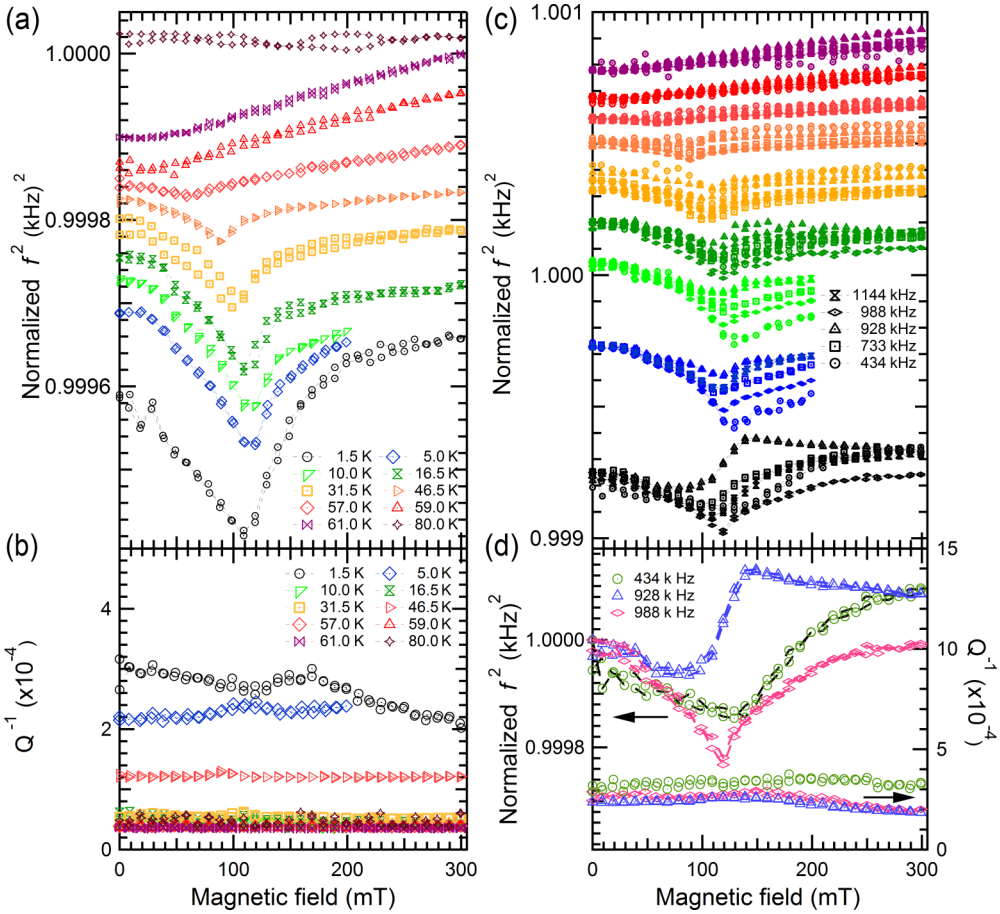

FIG. 4. Values of f^2 (normalized) and Q^{-1} as a function of magnetic field at selected temperatures. (a) 1144 kHz resonance. The f^2 values rescaled to give ~1 at the lowest temperature and then offset by some arbitrary amount up the y axis for clarity. The minimum in f^2 near 100 mT at 1.5 K shifts to lower fields with increasing temperature. (b) Q^{-1} for the same resonance as in (a) showing a small peak at ~95 mT/46.5 K,110 mT/5 K,~160 mT/1.5 K. (c) The f^2 values for five different resonances, with rescaling as in (a). The general pattern of softening is the same as in (a) but differs in detail at different resonant frequencies. An additional, very weak anomaly appears to be present near 50 mT in some datasets (e.g., 5, 10, 16.5 K). (d) The f^2 and Q^{-1} data for three resonances at 1.5 K, showing details of the different patterns of evolution with colors representing different frequencies rather than different temperatures.

between the amount of softening and frequency, however, implying that the differences are not due to conventional effects of dispersion as might apply in the case of a thermally activated freezing process.

Figure 4(d) shows details of the field dependence of f^2 and Q^{-1} for three resonances at 1.5 K. This highlights the lack of correlations with frequency that might be attributed to conventional dispersion effects associated with anelastic softening and loss. It is more likely that the differences arise from the different combinations of elastic constants which determine the frequencies of each resonant mode of the crystal. Inspection of the patterns of variation in Fig. 4(c) suggests that the two limiting patterns at almost all temperatures are represented by the 434 and 928 kHz resonances, reflecting variations of $\frac{1}{2}(C_{11} - C_{12})$ and C_{44} (though not necessarily in that order). Some additional contribution, perhaps from K, may then account for the difference of the 988 kHz mode at 1.5 K [Fig. 4(d)]. The 928 and 988 kHz modes have a small increase in loss through the range of fields in which the relatively steep (but still very small) change in f^2 occurs, while there is no equivalent increase through the wider interval of softening/stiffening of the 434 kHz mode.

Values of $H_{f\,2\mathrm{min}}$, obtained by fitting a parabola to f^2 in a narrow interval near minima of the softening shown in Fig. 4(c), are given in Fig. 5. They are superimposed on the phase diagram from Fig. 1 to show a correlation between elastic softening and the locus of H_{c2}. Scatter of the $H_{f\,2\mathrm{min}}$ values around the H_{c2} line is not systematic with frequency and is again more likely to reflect different temperature dependences for the different combinations of elastic constants. A marked difference from the trend of H_{c2} occurs below ~4 K, however, and the steep drop in $H_{f\,2\mathrm{min}}$ occurs for all the resonances analyzed in detail.

Also added to the phase diagram in Fig. 5 is the variation of T_c with field, based on the locus of the kink in f^2 visible in Fig. 3(a). This kink occurs at ~61 K in zero field but shifts slightly to higher temperatures as the field is increased. It is ~3 K above the value of T_c from the sharp peak in the real part of the ac magnetic susceptibility reported by Qian *et al.* [24],

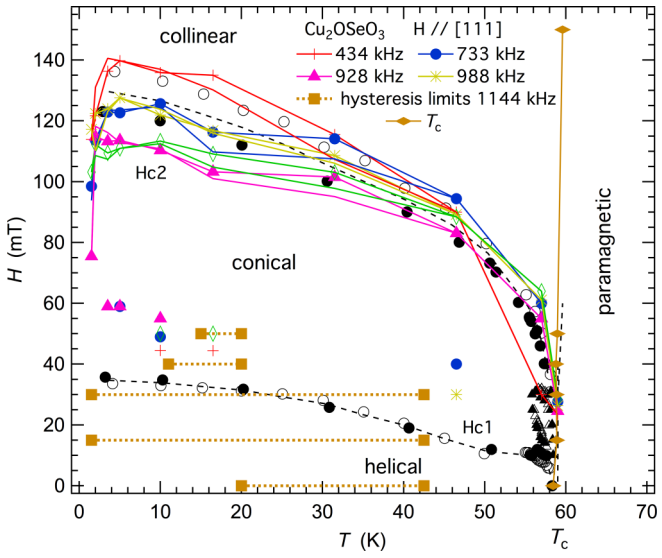

FIG. 5. Values of $H_{f\,2\mathrm{min}}$ (colored markers and solid lines) superimposed on data for H_{c1} and H_{c2} from Fig. 1. Values shown for T_c are 3 K below the temperature at which the pronounced kink occurs in f^2 [Fig. 3(a)]. Separate colored markers indicate the approximate position of slight softening with increasing field seen in f^2 data at low fields in Fig. 4(c). Limits of hysteresis seen in Fig. 6 are shown as filled squares joined by dotted lines.

but almost exactly where the susceptibility starts to increase steeply. Thus, it is obvious that the kink in $f^2(T)$ is related to the onset of magnetic ordering. Its field dependence can be qualitatively matched to the Curie-Weiss like temperature $T_0(H)$ found in magnetic measurements [24] if the temperature where the kink occurs is shifted by 3 K as shown in Fig. 5.

An additional subtle feature of the field dependences in Fig. 4(c) is a very slight dip in the trend of f^2 at low field strengths in some of the data. This is at the limit of experimental resolution but is present as a broad feature for enough resonances that it might be real. When plotted in Fig. 5, the approximate temperature and field values of this anomaly occur just above the expected locus of H_{c1}.

C. Hysteretic effects

Hysteresis effects are evident in the field-dependent variations of f^2, for example as differences between increasing and decreasing field at 16.5 and 31.5 K in Fig. 4(a). The effect is evident in the values of $H_{f\,2\mathrm{min}}$ for increasing and decreasing field, which are the same at temperatures of 46.5 K and above but are different at some lower temperatures. At temperatures of 31.5 K and below, there is tendency for the value of $H_{f\,2\mathrm{min}}$ to occur at a lower value when the applied field is being reduced compared with when it is being increased.

A complete picture of hysteretic effects with varying temperature is given in Fig. 6 for resonances with frequencies close to 1104 and 1144 kHz. This includes data collected with the applied field set at 220 mT, which is well outside the limits of the different phase boundaries below T_c in Fig. 5. In zero field, the most significant differences between heating and cooling for the 1144 kHz peak occur in the range ~20–42 K. In 15 and 30 mT fields, they occur between 1.5 and ~42 K, but at 40 and 50 mT, the ranges are restricted to ~10–20 K and ~15–20 K, respectively. These intervals have been added to Fig. 5 and fall in a similar range of the phase diagram to the small anomalies seen at low fields when varying temperature. No hysteresis has been seen below ~42 K at 150 mT, but a very slight effect is perhaps present when the field is 220 mT. This overall picture is the same for three other resonances that were analyzed (434, 928, 988 kHz).

Also apparent in data from the 1144 kHz peak are details of Q^{-1} which appear to show small variations between ~10 and ~42 K, but which do not obviously correlate with the hysteresis limits (Fig. 6). These are absent in all the data collected in a 220 mT field, which show only the kink in f^2 at T_c, the Debye loss behavior at ~42 K, and the increasing loss below ~10 K accompanied by very slight softening. Data from the 1104 kHz (Fig. 6) are generally similar apart from two details. Firstly, the very slight loss peak evident at T_c in Fig. 3(a) is clear but is weakest in zero field and absent in 220 mT. Secondly, the hysteresis in f^2 is barely detectable.

IV. DISCUSSION

For a material which nominally retains cubic lattice geometry throughout a wide field of T-H space (i.e., without any detectable coupling of magnetic ordering with strain), Cu_2OSeO_3 displays a remarkable diversity of subtle elastic and anelastic anomalies. The features of the elastic properties that most obviously correlate with the known T-H phase diagram are the small increase in elastic stiffness with falling temperature through T_c and the weak minima in stiffness which correlate approximately with H_{c2}. Entirely unexpected features are the peak in acoustic loss at ~42 K, which appears to correlate with a change from reversible elastic behavior at higher temperatures to irreversible behavior at lower temperatures, and marked changes in properties below ~10 K. Hysteresis is likely to be a signal of changes in the configuration of a domain structure which evolves differently during heating and cooling or during increasing and then decreasing external field. Effects which can be understood from the perspective of static coupling will be considered first.

A. Static coupling

In the case of a cubic-rhombohedral transition, the symmetry-breaking shear strain is $e_4(=e_5=e_6)$. For a transition driven by magnetic ordering this would be expected to couple with the magnetic order parameter M according to $\lambda_1 e_4 M^2$ to give improper ferroelastic behavior. If the coupling coefficient λ_1 is significantly different from zero and the relaxation time is small compared with the frequency of the applied stress, a steplike softening would be expected in C_{44} with lowering of temperature through T_c. No measurable distortion from cubic lattice geometry has yet been seen in Cu_2OSeO_3, so the absence of this steplike softening is consistent with λ_1 being small.

The next coupling term permitted by symmetry is $\lambda_2 e_4^2 M^2$ which would lead to stiffening or softening, depending on the sign of λ_2, even if $e_4 = 0$. C_{44} would be expected to vary as $C_{44}^o + 2\lambda_2 M^2$, where C_{44}^o is the elastic constant of the

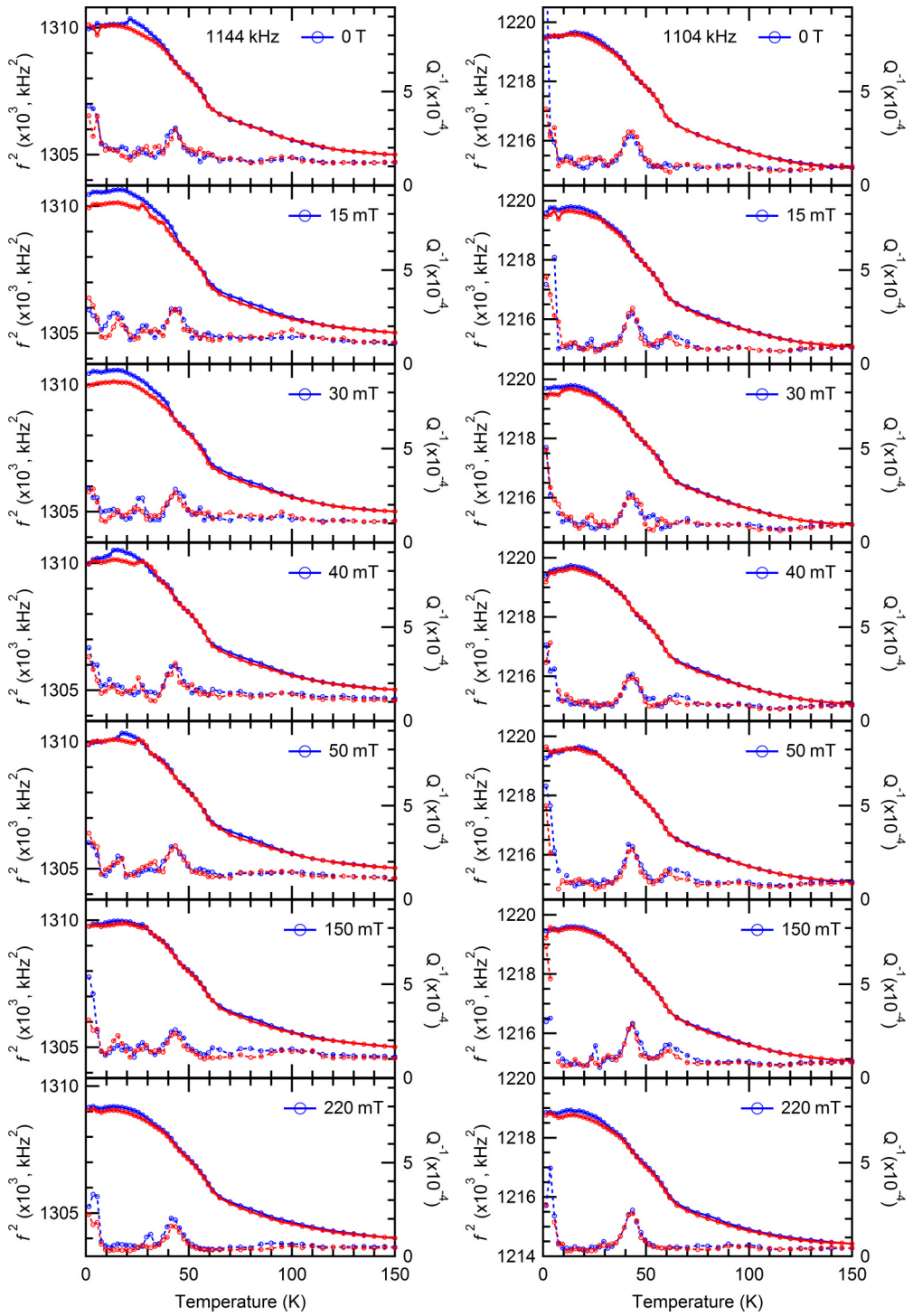

FIG. 6. Results for f^2 and Q^{-1} from detailed analysis of resonances with frequencies near 1104 (left) and 1144 kHz (right). Original spectra collected by starting at 1.5 K, applying the specified field, and then following a sequence of heating (red) followed by cooling (blue) as set out in the Appendix.

parent cubic structure [25]. The same argument applies for tetragonal and orthorhombic shear strains, so the same form of softening or stiffening is expected for $\frac{1}{2}(C_{11} - C_{12})$. On this basis, the difference $\Delta|f^2|$ between a baseline extrapolated to below T_c using the expression of Varshni [26] and data for the magnetic structure are expected to vary with M^2. Independent measures of the temperature dependence of the magnetic order parameter are compared with $\Delta|f^2|$ in Fig. 7 and confirm this relationship, at least for temperatures between T_c and ~42 K. The magnetic data are intensities of a reflection due to the helical order seen by small-angle neutron scattering [5], which are expected to scale with M^2, and the square of the saturation

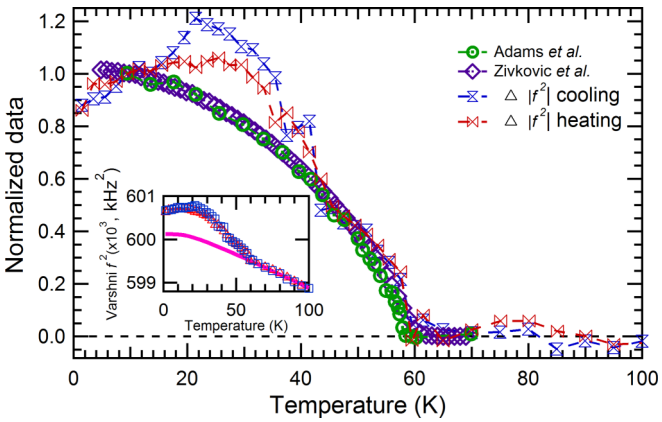

FIG. 7. Comparison of the excess elastic stiffening, $\Delta|f^2|$, below $T_c \approx 60$ K with the intensity of a superlattice reflection which varies with M^2 (green data points, from Fig. 4(a) of Adams *et al.* [5]) and M^2 directly, as measured in a field of 100 mT aligned parallel to [110] (purple squares, data from Fig. 3 of Živković *et al.* [27]). Magnetic data normalized to 1 at 10 K, and $\Delta|f^2|$ data (619 kHz resonance for cooling, 592 kHz for heating) scaled to show that they are permissive of $\Delta|f^2| \propto M^2$, at least between 60 and ~42 K. Pink line in insert shows the fit of the Varshni equation for the baseline used to obtain values of $\Delta|f^2|$.

magnetization measured in a 100 mT field parallel to [110] (Ref. [27]).

An additional contribution to the change in f^2 might have come from changes in piezoelectric and piezomagnetic coefficients through T_c. It is known that the mechanical resonance frequencies of a piezoelectric crystal depend both on the elastic moduli and, to a very much smaller extent, on the piezoelectric coefficients [28–30]. Under point group 23, both piezoelectricity and piezomagnetism are allowed [1,6], but the magnitudes remain to be quantified.

The patterns of softening and stiffening with increasing magnetic field at constant temperature are not so easily explained without information on the form of variation of order parameters for the collinear and conical magnetic structures. An additional factor may be the electric polarization that develops with increasing field [2,3,6,9], because coupling of the underlying crystal structure with electric dipoles is likely to be stronger than coupling with spins. The effect of the applied field can be understood, in qualitative terms at least, as first reorienting the helical **q** vector and then inducing a conical component parallel to the field, with the magnitude of the electric polarization scaling with the square of the magnetization [2,3,9]. Evidence for weak strain coupling is provided by the first (i.e., at ~50 mT) small variations in f^2 with increasing field at constant temperature (Fig. 4). There are also hysteretic effects in f^2 at about the same conditions of H and T (Figs. 5 and 6), and these are most likely due to changes in domain configurations, either of the helical phase, the conical phase, or both. Differences between the 1104 and 1144 kHz peaks (Fig. 6) suggest that different shear elastic constants do not vary in an identical manner and, hence, that the form and/or strength of coupling with the electric polarization and magnetic moment are also different for the related shear strains. Elastic compliances are, in effect, susceptibilities with respect to strain and, if there is strong coupling between an electric dipole and strain, should show similar behavior to the dielectric constant [31]. It would be of interest, therefore, to examine the effect of magnetic field on the real and imaginary components of the dielectric constant of Cu_2OSeO_3.

Compared with the only slight correlation of anomalies in f^2 with the likely location of H_{c1}, the distinct anomalies at higher fields are more definitely associated with H_{c2}. In other words, strain coupling associated with the conical-collinear transition is stronger than at the helical-conical transition. Variations in the locus of $H_{f\,2\min}$ between different resonances show that the coupling of strain with the order parameter(s) differs for different symmetry-adapted strains.

B. Anelastic relaxation

Mobility of ferroelastic twin walls under the influence of an externally applied stress would be expected to give rise to a steep increase in Q^{-1}, followed by a plateau of high acoustic loss, as is typical of improper ferroelastic transitions in perovskites [21]. That this is not seen in Cu_2OSeO_3 is consistent with weak/absent coupling of shear strains with the driving order parameter. There is evidence in Figs. 3(a) and 6 for a very weak loss peak at T_c, but this is not seen in data from all the resonances, implying that it is a relaxational response of only one of the possible symmetry-adapted strains. Given the lack of evidence for linear-quadratic coupling with any shear strain, the most likely relaxation is of a volume strain. Elastic stiffening, diffraction, and magnetization measurements (Fig. 7) all point to the transition being continuous, so that the loss mechanism is not expected to be due to mobility of interfaces between coexisting low- and high-symmetry forms. Levatic *et al.* [32] observed a distinct loss peak near T_c in ac magnetic data collected at ~1 kHz. This was negligibly small in zero field but increased markedly with increasing field. No equivalent field dependence has been seen for the acoustic loss peak reported here, which would again be consistent with weak magnetoelastic coupling.

The well-developed peak in Q^{-1} at ~42 K has the typical form of Debye loss associated with freezing of some defect which couples with strain. A phase transition can probably be ruled out because none of the phase diagrams reported in the literature (e.g., Refs. [2,5]) show any evidence of anomalies in structure or physical properties in this vicinity. Thermally activated relaxational processes with relaxation time τ at temperature T, activation energy E_a, and the reciprocal of the attempt frequency τ_o would conform to $\tau = \tau_o \exp(E_a/\mathrm{RT})$. The Debye peak itself is expected to depend on the angular frequency $\omega\,(=2\pi f)$ of an applied stress according to

$$Q^{-1} = \Delta \frac{\omega\tau}{1+\omega^2\tau^2}, \tag{1}$$

and the value of Δ in the case of a standard linear solid is given by

$$\Delta = \frac{C_U - C_R}{C_R} \quad (\text{for } C_U - C_R \ll C_R). \tag{2}$$

C_U is the relevant elastic modulus for the unrelaxed state, and C_R is the elastic modulus of the relaxed state [33]. The

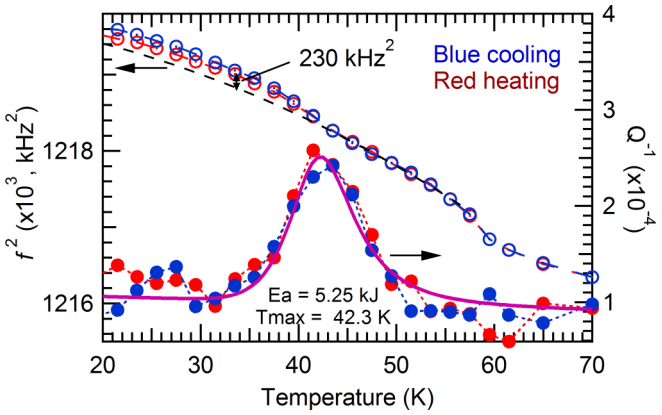

FIG. 8. Fit of Eq. (3) shown for the Debye loss peak. The dashed line is a fit to data between ~45 and ~55 K as a guide to the eye to show the approximate magnitude of anelastic stiffening associated with the Debye freezing process. This stiffening amounts to ~230 kHz^2, which is a change of ~0.019 %.

maximum value of Q^{-1}, Q_m^{-1}, occurs at temperature T_m and is equal to $\Delta/2$. A single peak measured as a function of temperature at approximately constant frequency can be described by [34,35]

$$Q^{-1}(T) = Q_m^{-1}\left\{\cosh\left[\frac{E_a}{Rr_2(\beta)}\left(\frac{1}{T}-\frac{1}{T_m}\right)\right]\right\}^{-1}, \quad (3)$$

where $r_2(\beta)$ is a width parameter which arises from any spread in relaxation times for the dissipation process. The width of a peak measured as a function of temperature at constant frequency is determined essentially by the values of E_a and $r_2(\beta)$. Fits of Eq. (3), including an estimate of the baseline, are shown in Fig. 8, with $E_a/r_2(\beta) = 5.3$ kJ mol^{-1}, $Q_m^{-1} = 0.000152$, $T_m = 42.3$ K. The value of Δ in Eq. (1) obtained by inserting the fit value of Q_m^{-1} is 0.03%, corresponding to a stiffening of 0.015%. This is consistent with the observed variations of f^2 shown in Fig. 8, which shows an offset of ~0.019 %. If the dissipation process involves a single relaxation time, the value of β is 0 and the value of $r_2(\beta)$ is 1. In this case Eq. (3) gives $\tau_o \approx 3.07 \times 10^{-14}$ s since the resonance peak used to determine Q^{-1} was at $f(=2\pi/\tau) \approx$ 1104 kHz.

The helical phase is known to contain domains with different orientations of the **q** vector [4,5,36], but in the absence of any shear strain below T_c, the domain walls would not be ferroelastic. The loss peak at ~42 K is independent of magnetic field strength and is seen as a function of temperature in fields up to at least 220 mT (Fig. 6). In the stability fields of the conical and ferromagnetic structures, only single domains exist because the net magnetic moment is aligned parallel to the applied field, and it follows that freezing of ferroelastic twin walls cannot be the cause. Rather, there must be some defect which is coupled with shear strain, which relaxes on a time scale of $\sim 10^{-6}$ s at ~42 K ($\omega\tau = 1$) and which experiences an activation energy barrier of ~5 kJ mol^{-1}. A possible analogy is provided by the incommensurate structure of $Pr_{0.48}Ca_{0.52}MnO_3$ (PCMO), for which a similar peak was found at ~72 K with $E_a \approx 7$ kJ mol^{-1}, $\tau_o \approx 10^{-11}$ s, $\Delta \approx 3\%$ [37]. This was attributed to the influence of a shear stress on the repeat distance of the incommensurate modulation, with the activated step being diffusion of polarons. The analogy is not exact, however, because the incommensurate transition in PCMO is coupled to a significant shear strain. A very similar anelastic loss occurs in $YBa_2Cu_3O_{6+x}$ ($E_a \sim 7.3$ kJ mol^{-1}, $\tau_o \sim 10^{-13}$s, $T_m \sim$ 40–60 K at ~2–22 kHz) and has also been attributed to movement under external stress of polarons [38]. Cu_2OSeO_3 is an insulator, but the idea of a relaxation cloud around some crystallographic or electronic defect remains a possibility. Relatively high but nearly constant values of Q^{-1} occur with varying field at 46.5 K [Fig. 4(b)], consistent with the lack of field dependence for the Debye loss peak when measured as a function of temperature in different fields. The defect responsible is coupled with shear strain but appears not to be magnetic.

It has recently been proposed that the nanoscale dynamics of the helimagnetic phase of FeGe are controlled by depinning and motion of magnetic edge dislocations [39]. If this is correct, their coupling with the underlying lattice is also likely to be important, and the present case of Cu_2OSeO_3 shows how the pinning and unpinning processes might be characterized.

C. Hysteresis

Between T_c and T_m, values of the resonance frequencies are the same during heating and cooling, while below T_m they are generally very slightly lower during heating from 1.5 K than during subsequent cooling [Fig. 3(c)]. There are also some more abrupt changes, but it appears that the hysteretic effects and the defect freezing below ~42 K are related. The small but systematic differences between increasing and decreasing field, seen particularly at 31.5 and 16.5 K but not at 46.5 K and above, are also consistent with this (Fig. 4). Some aspect of the magnetic microstructure presumably gets reset at the lowest temperatures when temperature is changed and in the stability field of the collinear structure when field is changed. This does not relax fully back to its original configuration when the temperature is below T_m, but above 42 K there is sufficient thermal energy for an equilibrium configuration to return.

The most likely aspects of the microstructure responsible for the irreversible changes are the boundaries between domains with different orientations of the helical or conical structures. These would have the potential to acquire different configurations according to the thermal history of the sample, particularly if they could also be pinned by the defects. A single crystal containing different proportions of magnetic domains will have different bulk elastic constants if there are small changes associated with breaking the magnetic symmetry. It is notable that the magnitude of the irreversible changes is markedly lower when heating and cooling in a field of 150 and 220 mT. This is well within the stability field of the collinear structure where there is likely to be only one magnetic domain orientation. Between ~10 and ~40 K, there are small variations in Q^{-1} which could be associated with the dynamics of changing twin wall orientations or pinning of different configurations, but these also essentially disappear in a 220 mT field (Fig. 6). A corollary of this is that cooling to 1.5 K appears to result in hysteretic effects, as though there

is a change in either the configuration of twin domains or the magnetic structure stable at the lowest temperatures.

D. Low-temperature anomalies

There appear to be no other reports of significant anomalies in physical properties for Cu_2OSeO_3 below ∼10 K. Bos *et al.* [1] had originally reported a change in the sign of the dielectric anomaly, relative to extrapolated values of the parent structure, at ∼20 K, but measurements to higher temperatures (e.g., Refs. [6,27]) showed that this depends on how the extrapolation is made. Similarly, peaks apparently existing in Raman spectra only below ∼20 K [15] were later shown to be present up to room temperature [40]. In the absence of other evidence it is not possible to conclude whether there is another phase transition or just some additional relaxation, but the steep drop in $H_{f\,2\mathrm{min}}$ at the lowest temperatures (Fig. 5) suggests, at least, that there is a relationship with the changing magnetic structure at H_{c2}.

The characteristic features of the elastic and anelastic anomalies are a steep increase in acoustic loss below ∼10 K and a change in trend from the normal pattern of stiffening with falling temperature to softening. There are variations in the magnitude of the maximum observed values of Q^{-1} as a function of field [Figs. 4(b) and 6], implying that the relaxational process responsible involves some magnetoelastic coupling. The anomalies extend up to 220 mT, however, so they are unlikely to be due to domain wall motion. Below ∼4.2 K the sample chamber must contain a small amount of liquid helium which, if preferentially coating the sample, might influence the resonant frequencies and acoustic loss. However, the same effect has not been observed with samples of other materials under the same conditions (e.g., Ref. [23]), and it is more likely that the low-temperature anomaly is due to some change in the crystal structure or magnetic configuration of the sample.

V. CONCLUSIONS

In spite of there not being any evidence of a symmetry-breaking shear strain, small elastic anomalies accompanying the magnetic phase transitions show that Cu_2OSeO_3 displays a variety of elastic and magnetoelastic behavior in addition to the magnetic and magnetoelectric properties that have already been described in the literature. As a function of temperature at all fields up to at least 220 mT, stiffening of the single-crystal elastic constants by up to ∼0.1% scales with the square of the magnetic order parameter, as would be expected if there is coupling with shear strains of the form $\lambda e^2 M^2$. The implications of this biquadratic strain-coupling mechanism are not clear, but it is evidently a significant feature of the helimagnetic structures in Cu_2OSeO_3. Small anomalies in the shear elastic constants associated also with the metamagnetic transitions, most obviously at H_{c2}, differ in form for different mechanical resonances and imply different coupling of the magnetic order parameter(s) with shear strains. By way of contrast, we have found evidence, in the form of classic anelastic loss behavior through the stability fields of all three magnetic structures, of some nonmagnetic defect which is coupled with shear strain and which plays a role in pinning of the magnetic microstructure below ∼42 K. Such pinning could account for the hysteresis effects at low fields and low temperatures if they are due to changes in configuration of magnetic domains. The cause of the additional unexpected anelastic anomaly at temperatures below ∼10 K is not understood but seems to have a significant influence on the relative stabilities of the conical and collinear structures at H_{c2}.

ACKNOWLEDGMENTS

RUS facilities have been established and maintained through grants from the Natural Environment Research Council and the Engineering and Physical Sciences Research Council of Great Britain to M.A.C., which are gratefully acknowledged (Grants No. EP/I036079/1, No. NE/B505738/1, and No. NE/F17081/1). This paper was supported specifically under Grant No. EP/I036079/1.

APPENDIX: SEQUENCE OF DATA COLLECTIONS WITH RESPECT TO CHANGING TEMPERATURE AND MAGNETIC FIELD

The first line in Table I indicates the first experiment: starting with a field of 0 T and temperature 294 K, the sample was cooled to 1.5 K. The next run was also in zero field, starting at 1.5 K, heating to 150 K, and cooling to 1.5 K. A field of 30 mT was then applied, and the sample was heated from 1.5 to 150 K, followed by cooling back to 1.5 K. Successive lines through Tables I–III give the full thermal/magnetic history of the sample.

TABLE I. Sequence of variable temperature at fixed magnetic field.

Field (mT)	Initial temperature (K)	Middle temperature (K)	Final temperature (K)
0	294		1.5
0	1.5	150	1.5
30	1.5	150	1.5
40	1.5	150	1.5
50	1.5	150	1.5
15	1.5	150	1.5
150	1.5	150	1.5
220	1.5	150	1.5

TABLE II. Sequence of variable field at fixed temperature.

Temperature (K)	Initial field (mT)	Middle field (mT)	Final field (mT)
1.5	0	300	0
16.5	0	300	0
31.5	0	300	0
46.5	0	300	0
57	0	300	0
59	0	300	0
61	0	300	0
80	0	300	0
200	0	300	0

TABLE III. Final sequence, including hysteresis loops between 1000, −1000, and 1000 mT, although the data from these are not reported here.

Temperature (K)	Initial field (mT)		Middle field (mT)		Final field (mT)
16.5	0	1000	−1000	1000	0
59	0	1000	−1000	1000	0
70	0	1000	−1000	1000	0
10	0		200		0
5	0		200		0
3.5	0		200		0

[1] J.-W. G. Bos, C. V. Colin, and T. T. M. Palstra, Phys. Rev. B **78**, 094416 (2008).

[2] S. Seki, X. Z. Yu, S. Ishiwata, and Y. Tokura, Science **336**, 198 (2012).

[3] S. Seki, S. Ishiwata, and Y. Tokura, Phys. Rev. B **86**, 060403 (2012).

[4] S. Seki, J.-H. Kim, D. S. Inosov, R. Georgii, B. Keimer, S. Ishiwata, and Y. Tokura, Phys. Rev. B **85**, 220406 (2012).

[5] T. Adams, A. Chacon, M. Wagner, A. Bauer, G. Brandl, B. Pedersen, H. Berger, P. Lemmens, and C. Pfleiderer, Phys. Rev. Lett. **108**, 237204 (2012).

[6] M. Belesi, I. Rousochatzakis, M. Abid, U. K. Rößler, H. Berger, and J.-Ph. Ansermet, Phys. Rev. B **85**, 224413 (2012).

[7] J. S. White, K. Prša, P. Huang, A. A. Omrani, I. Živković, M. Bartkowiak, H. Berger, A. Magrez, J. L. Gavilano, G. Nagy, J. Zang, and H. M. Rønnow, Phys. Rev. Lett. **113**, 107203 (2014).

[8] A. A. Omrani, J. S. White, K. Prša, I. Živković, H. Berger, A. Magrez, Ye-Hua Liu, J. H. Han, and H. M. Rønnow, Phys. Rev. B **89**, 064406 (2014).

[9] E. Ruff, P. Lunkenheimer, A. Loidl, H. Berger, and S. Krohns, Sci. Rep. **5**, 15025 (2015).

[10] M. Mochizuki and S. Seki, J. Phys. Condens. Matter **27**, 503001 (2015).

[11] K. H. Miller, X. S. Xu, H. Berger, E. S. Knowles, D. J. Arenas, M. W. Meisel, and D. B. Tanner, Phys. Rev. B **82**, 144107 (2010).

[12] J. S. White, I. Levatic, A. A. Omrani, N. Egetenmeyer, K. Prša, I. Živković, J. L. Gavilano, J. Kohlbrecher, M. Bartkowiak, H. Berger, and H. M. Rønnow, J. Phys. Condens. Matter **24**, 432201 (2012).

[13] Y. Okamura, F. Kagawa, M. Mochizuki, M. Kubota, S. Seki, S. Ishiwata, M. Kawasaki, Y. Onose, and Y. Tokura, Nat. Commun. **4**, 2391 (2013).

[14] M. C. Langner, S. Roy, S. K. Mishra, J. C. T. Lee, X. W. Shi, M. A. Hossain, Y.-D. Chuang, S. Seki, Y. Tokura, S. D. Kevan, and R. W. Schoenlein, Phys. Rev. Lett. **112**, 167202 (2014).

[15] V. P. Gnezdilov, K. V. Lamonova, Yu. G. Pashkevich, P. Lemmens, H. Berger, F. Bussy, and S. L. Gnatchenko, Low Temp. Phys. **36**, 550 (2010).

[16] M. Belesi, I. Rousochatzakis, H. C. Wu, H. Berger, I. V. Shvets, F. Mila, and J. P Ansermet, Phys. Rev. B **82**, 094422 (2010).

[17] C. L. Huang, K. F. Tseng, C. C. Chou, S. Mukherjee, J. L. Her, Y. H. Matsuda, K. Kindo, H. Berger, and H. D. Yang, Phys. Rev. B **83**, 052402 (2011).

[18] V. A. Sidorov, A. E. Petrova, P. S. Berdonosov, V. A. Dolgikh, and S. M. Stishov, Phys. Rev. B **89**, 100403 (2014).

[19] H. C. Wu, K. D. Chandreasekhar, T. Y. Wei, K. J. Hsieh, T. Y. Chen, H. Berger, and H. D. Yang, J. Phys. D **48**, 475001 (2015).

[20] A. Migliori and J. L. Sarrao, *Resonant Ultrasound Spectroscopy: Applications to Physics, Materials Measurements and Nondestructive Evaluation* (Wiley, New York, 1997).

[21] M. A. Carpenter, J. Phys. Condens. Matter **27**, 263201 (2015).

[22] R. E. A. McKnight, M. A. Carpenter, T. W. Darling, A. Buckley, and P. A. Taylor, Am. Min. **92**, 1665 (2007).

[23] J. A. Schiemer, L. J. Spalek, S. S. Saxena, C. Panagopoulos, T. Katsufuji, A. Bussmann-Holder, J. Köhler, and M. A. Carpenter, Phys. Rev. B **93**, 054108 (2016).

[24] F. Qian, H. Wilhelm, A. Aqeel, T. T. M. Palstra, A. J. E. Lefering, E. H. Brück, and C. Pappas, Phys. Rev. B **94**, 064418 (2016).

[25] M. A. Carpenter and E. K H. Salje, Eur. J. Mineral. **10**, 693 (1998).

[26] Y. P. Varshni, Phys. Rev. B **2**, 3952 (1970).

[27] I. Živković, D. Pajić, T. Ivek, and H. Berger, Phys. Rev. B **85**, 224402 (2012).

[28] I. Ohno, Phys. Chem. Minerals **17**, 371 (1990).

[29] M. L. Dunn, H. Ledbetter, and P. Heyliger, J. Acoust. Soc. Am. **99**, 2594 (1996).

[30] H. Ogi, N. Nakamura, K. Sato, M. Hirao, and S. Uda, IEEE Trans. Ultrason. Ferroelectr. Freq. Control **50**, 553 (2003).

[31] M. A. Carpenter, J. F. J. Bryson, G. Catalan, S. J. Zhang, and N. J. Donnelly, J. Phys. Condens. Matter **24**, 045902 (2012).

[32] I. Levatic, V. Šurija, H. Berger, and I. Živković, Phys. Rev. B **90**, 224412 (2014).

[33] A. S. Nowick and B. S. Berry, *Anelastic Relaxation in Crystalline Solids* (Academic, New York, 1972).

[34] M. Weller, G. Y. Li, J. X. Zhang, T. S. Ke, and J. Diehl, Acta Metall. **29**, 1047 (1981).

[35] Edited by R. Schaller, G. Fantozzi, and G. Gremaud, *Mechanical Spectroscopy, with Applications to Materials Science, Proceedings of the Summer School Q-1 2001*, Materials Science Forum, Vol. 366–368 (Trans Tech Publications, Switzerland, 2001).

[36] J. Rajeswari, P. Huang, G. F. Mancini, Y. Murooka, T. Latychevskaia, D. McGrouther, M. Cantoni, E. Baldini, J. S. White, A. Magrez, T. Giamarchi, H. M. Ronnow, and F. Carbone, Proc. Natl. Acad. Sci. USA **112**, 14212 (2015).

[37] M. A. Carpenter, C. J. Howard, R. E. A. McKnight, A. Migliori, J. B. Betts, and V. R. Fanelli, Phys. Rev. B **82**, 134123 (2010).

[38] G. Cannelli, R. Cantelli, F. Cordero, F. Trequattrini, and M. Ferretti, Phys. Rev. B **54**, 15537 (1996).

[39] A. Dussaux, P. Schoenherr, K. Koumpouras, J. Chico, K. Chang, L. Lorenzelli, N. Kanazawa, Y. Tokura, M. Garst, A. Bergman, C. L. Degen, and D. Meier, Nat. Comm. **7**, 12430 (2016).

[40] V. S. Kurnusov, V. P. Gnezdilov, V. V. Tsapenko, P. Lemmens, and H. Berger, Low Temp. Phys. **38**, 489 (2012).